Compact Robotic Gripper With Tandem Actuation for Selective Apple Harvesting

Alejandro Velasquez, Cindy Grimm, and Joseph R. Davidson

***Abstract*—One of the primary reasons robotic apple harvesting is a challenging manipulation problem is the cluttered tree canopy. An effective harvesting gripper should i) be compact to minimize collisions with the canopy, ii) offer a compliant grasp to prevent bruising; and iii) hold the fruit securely to counteract forces during picking. Much of the prior work has used single-mode grippers (suction or fingers), which are often compliant but have low grasp strength (suction), or have a strong grasp but a large form factor (fingers). We present a compact robotic gripper that combines the benefits of both. It first uses an array of soft suction cups to gently attach to the fruit, then deploys three telescoping fingers that sweep away obstacles and pivot inward to secure the grasp. We analyze the finger design for its ability to sweep clutter and maintain a tight grasp, and we measure grasp strength across suction-only, fingers-only, and combined (tandem) actuation modes. Tandem mode consistently provides a grasp that can counter typically observed fruit detachment forces. Using an apple proxy, we test the gripper's performance in cluttered scenarios, achieving over 96% pick success with an ideal controller. Finally, we validate the gripper in a commercial apple orchard, achieving an 81% pick success rate.**

***Index Terms*—Agriculture robotics, Grasping, End effectors, Mechanism design.**

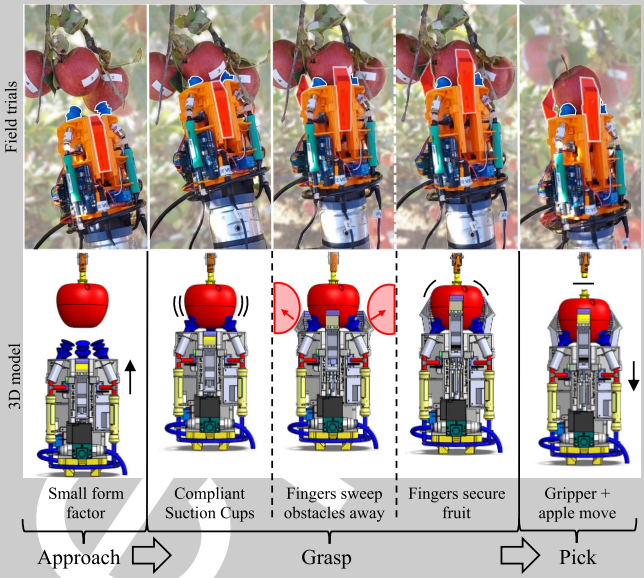

Fig. 1. From left to right. *Approach:* The gripper approaches the fruit with a small form factor to reduce collisions. *Grasp:* An initial compliant grasp with suction cups (blue) is followed by a grasp with cam-driven fingers (red in field trial images) that wedge between neighboring fruit. *Pick:* The apple is secured in the gripper during the picking motion.

I. Introduction

MOST fresh market fruits and vegetables are picked by the human hand. In many parts of the world, rising costs and labor shortages threaten the long-term economic sustainability of manually harvesting these specialty crops [1], [2]. While there have been decades of research on robotic harvesting and many advances in computing, sensors, and deep learning, there are few, if any, selective robotic harvesting systems that are commercially available to growers.

Robotic harvesting presents several challenges. First, the environment is highly unstructured: plant canopies often include heavy occlusions, clutter, and clusters of touching fruit. Second, environmental mechanics vary widely by crop and cultivation system, with soft vegetation like leaves interspersed among rigid elements such as limbs, trellis wires, and irrigation lines. Fruit are also free-floating and tend to swing when pushed. Third, while fruit are easily damaged, detachment requires substantial force [3]. For example, in apple harvesting, detachment force depends on the picking pattern [4], [5], [6]; linear pulling yields the highest forces. Other patterns (e.g., rotate, bend, and pull) reduce the required force and mitigate damage, but executing them demands that the gripper maintain a strong hold against forces coming from different directions. Addressing all of these challenges with a single robotic gripper is difficult. Most Selective Apple Harvesting (SAH) grippers use a single actuation mode—either finger-based or suction-based—each with inherent limitations. Suction grippers offer a compact form factor (gripper-to-fruit cross-section ratio) but often require strong vacuum to achieve the necessary detachment force and are less effective under shear loads from non-linear picking motions. Finger-based designs, while capable of withstanding lateral forces, typically have a wide opening span that increases the risk of collisions in cluttered canopies, leading to picking failures. *Our approach combines both actuation modes—suction and fingers—into a single, integrated design, replacing the traditional finger design with a cam-driven one with a minimal form factor.*

Our robotic gripper (Fig. 1) includes an array of three small, compliant suction cups which attach to the fruit. This array

Received 3 May 2025; accepted 22 August 2025. Date of publication 10 September 2025; date of current version 16 September 2025. This letter was recommended for publication by Associate Editor N. Lawrance and Editor G. Loianno upon evaluation of the reviewers' comments. This work was supported in part by USDA-NIFA under Award 2023-67021-38908 and in part by Washington Tree Fruit Research Commission. *(Corresponding author: Joseph R. Davidson.)*

The authors are with Collaborative Robotics and Intelligent Systems (CoRIS) Institute, Oregon State University, Corvallis, OR 97331 USA (e-mail: velasale@oregonstate.edu; cindy.grimm@oregonstate.edu; joseph.davidson@oregonstate.edu).

This article has supplementary downloadable material available at https://doi.org/10.1109/LRA.2025.3608635, provided by the authors.

Digital Object Identifier 10.1109/LRA.2025.3608635

IEEE Robotics and Automation Letters (RA-L) paper, presented at ICRA 2026, Vienna, Austria. Cite as RA-L paper.

has a small form factor (a cross section similar to the size of the fruit) to minimize collisions, while the compliance and suction minimize the likelihood that the fruit will be pushed away [7]. After suction is achieved, three telescoping fingers then extend outwards, pushing away obstacles and securely gripping the fruit for picking. While we designed our gripper for apple harvesting, the concept of tandem actuation with suction and telescoping/sweeping fingers could be extended to other types of fruits and vegetables.

We structured the letter as follows: Section II reviews finger-, suction-, and tandem-based gripper designs, highlighting key challenges. Section III presents our gripper and a static model for analyzing its strength in finger mode (the suction design is detailed in [7]). Section IV outlines experiments measuring grasp strength across varying apple poses and disturbance forces. Section V compares results across different actuation modes and shows that tandem actuation yields significantly higher strength (40 N), well above typical detachment forces. Our static model is able to predict the gripper grasp strength across the experiments. We also demonstrate robust in-lab grasps in clutter using a physical apple proxy [8]. Finally, we validate the gripper in a commercial orchard using an ideal controller and pull-back picking motion.

In summary, our contributions are the following: *(1) A tandem actuation gripper* that has two behaviors: i) compliant attachment to the fruit via suction; and ii) secure, stable grasping of the fruit using fingers. *(2) A cam-driven finger mechanism* with two deployment regions. The first region uses wedge-shaped finger pads to sweep obstacles away from the target fruit, and the second region clamps the fruit, using mechanical advantage to maintain that grasp and withstand Fruit Detachment Force (FDF) during harvesting.

II. Related Work

Of the grippers developed for agriculture, about 85% were designed for pick-and-place applications, and only around 15% specifically address selective fruit harvesting [9]. As mentioned earlier, SAH presents unique challenges: grippers must be compliant to adapt to natural variability and strong enough to detach the fruit. Recent work typically addresses these demands using passive compliant fingers, suction cups, or a tandem combination of both.

A. Finger-Based Grippers

Finger-based grippers for SAH typically use soft actuators, tendon-driven mechanisms, or flexible structural designs such as compliant-linkages or fin-ray fingers. Soft actuators, usually silicone-cast with internal cavities, bend inward when pressurized with fluid (e.g., air). Hohimer et al. [10] evaluated a three-finger 3D-printed soft gripper in a commercial orchard, achieving pull forces up to 100 N, sufficient for apple detachment. However, clustered fruit caused most failures (37%) due to gripper size and collisions. Precision control is also difficult due to air compressibility [11], prompting exploration of alternative actuators. Flexible structural designs use motor-driven fingers with base pivots and crossbeam supports for added stability. Compliant-linkage fingers contact at the tip [12], while fin-ray fingers wrap around fruit to improve grip and pressure distribution. Chen et al. [13] developed a three-finger fin-ray gripper with pressure sensing for slip control, achieving a 43 N pull force and 80% success in 25 bruise-free trials. Fin-ray designs may also enable indirect force estimation via visual deformation tracking [14]. Despite their adaptability, finger-based grippers face challenges: collisions during approach, wide spans ($2-3\times$ the gripper body), and fruit displacement during closure, which can all contribute to failed grasps.

B. Suction-Based Grippers

Suction-based grippers are an alternative that use vacuum to attach to fruit on contact. Some designs use a single cup; large cups provide a strong hold but only attach to fruit with larger radii and require rigid hoses that reduce robot maneuverability [3]. Smaller cups are often preferred. Hua et al. [15] reported higher picking success with a 33 mm cup compared to 43 mm, though smaller diameters reduce holding force. Arrays of smaller cups can compensate by increasing grip force and engagement area. Wang et al. [16] tested different cup numbers and sizes, achieving best results with a four-cup array (25 mm each). Arrays also allow embedding pressure sensors for pose correction. While suction handles tensile forces well, it struggles with shear forces during the pick.

C. Tandem-Based Grippers

A common combined setup uses tendon-driven or pressurized fingers integrated with a suction cup on the palm [17], [18], [19]. In these designs, the suction cup maintains fruit attachment during finger closure, while the fingers help stabilize the suction grip under various motion patterns. However, such tandem solutions often suffer from wide gripper span during approach, limiting their applicability in dense orchard environments.

Altogether, achieving all the requirements of SAH in a single gripper remains a challenge. Grippers that are too compliant may lack the strength to detach the fruit, while those capable of applying sufficient force often have a bulky form factor. Furthermore, many designs are validated only under idealized pull conditions, without accounting for variations in fruit pose or detachment force direction.

III. Gripper Design

We consider design specifications related to the kinematic and dynamic challenges of fruit picking mentioned earlier. We tackle these specifications by combining two actuation modes that complement each other: compliant multi-bellow suction cups and cam-driven fingers. The first provides a robust initial attachment and the latter deploys from underneath the gripper's palm, sweeping obstacles away and securing the apple for further manipulation (i.e. the picking motion).

A. Design Specifications

Based on our review of the prior art, we considered the following design specifications for the gripper:

- *Form factor:* The gripper should have a cross-section similar in shape and size to the targeted fruit to minimize unintended collisions in the cluttered canopy.
- *In-hand sensing:* The gripper should have in-hand perception such as cameras and time-of-flight sensors to allow active fruit localization during the approach.
- *Grasp strength:* The gripper should: i) provide sufficient grasp strength to withstand the forces required to detach the

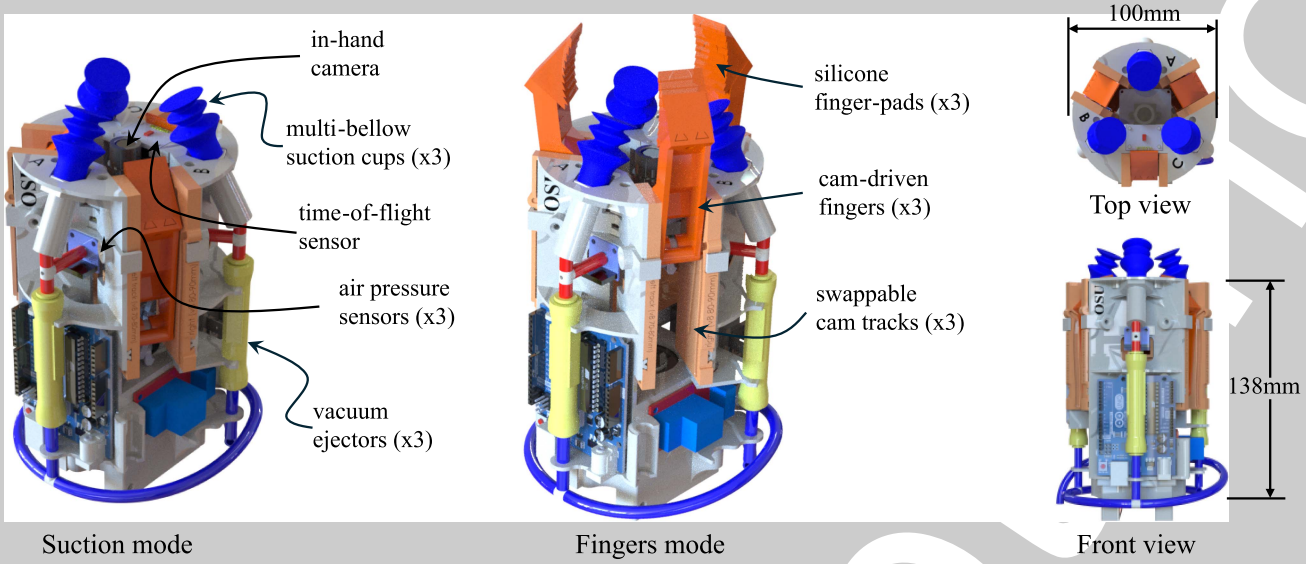

Fig. 2. Gripper render. *Left:* Suction mode from previous work [7] with fingers retracted and in-hand perception components labeled. *Middle:* Gripper with fingers deployed. *Top and bottom right:* Gripper's main dimensions with fingers retracted.

fruit; ii) maintain a stable grasp of the fruit during bending motions; and iii) accomplish i) and ii) without bruising the fruit with the grasp itself.

- *Robustness:* The gripper should be able to pick fruit in clusters (i.e. fruit that are touching), fruit adjacent to limbs, and fruit adjacent to other rigid obstacles such as trellis wires and irrigation lines.

B. Design Description

Actuation. Our gripper employs two actuation modes (Fig. 2). The first mode is suction with three compliant bellows suction cups instead of one (described in [7]). The multiple bellows arrangement has the benefits of increasing the likelihood of fruit attachment, creating an open field of view for perception sensors located in the center of the palm, and providing three contact points to help stabilize the fruit. The second actuation mode, which begins after suction is complete, is telescoping, cam-driven fingers that sweep outward from the gripper and provide a strong grasp to complete the picking motion (described in Section III-C).

Sensors. The gripper palm includes an in-hand camera (ELP High Speed USB Camera, 1080P) and a time-of-flight sensor (Adafruit VL53L0X) to enable visual servoing to the apple. Additionally, air pressure sensors (Adafruit MPRLS) are positioned near the intake of each suction cup to detect engagement and support air-pressure differential servoing. These servoing methods are not within the scope of this paper and are therefore not discussed further.

C. Cam-Driven Fingers

The primary motivation for the cam-driven mechanism is to create two different finger 'behaviors' with the same mechanism: *obstacle sweeping* and *fruit clamping*. The geometry of the cam paths defines the finger behaviors. Each finger has two pivot pins (inner and outer) that slide along the cam paths and define the finger pose (Fig. 3-*Left*). The cam paths are embedded into modular 3D-printed parts that can be easily for harvesting different types of fruit and fruit sizes. The actuator for the three coupled fingers is a stepper motor with a lead screw transmission.

First region: obstacle sweeping. This region of the path prioritizes moving the fingers along the sides of the fruit, following a curved path from underneath the gripper palm and up to the fruit equator (Fig. 3-*Middle*). During this motion, the fingers sweep obstacles (e.g., neighboring fruit, vegetation) away from the fruit with the outer side of wedge-shaped finger pads. We designed the paths using fit-point spline curves defined by control points and validated them in CAD. The control points for the outer path spline are (in mm): o_1 (6.3, 2.1), o_2 (7.6, 21.6), o_3 (7.5, 38.6), and o_4 (8.9, 60.5); and for the inner path spline: i_1 (17.0, 18.1), i_2 (14.5, 60.5), and i_3 (16.2, 78.3).

Second region: fruit clamping. The fingers secure the fruit when the inner pivot pin reaches the end of the inner path (i.e. is constrained by a hard stop at i_3), and the outer pivot pin transitions to the last section of the outer path with a radius $r_c = 19$ mm until it reaches the control point o_5 (4.0, 63.5). This results in a rotation of the finger around the inner pivot pin, securing the fruit with the inner side of the finger pads (Fig. 3-*Middle*). The finger pads are made from soft silicone (Dragon Skin^{TM} 20, Smooth-on Inc., USA) to avoid bruising the fruit and to increase friction. This region of the cam path prioritizes securing the fruit in a tight grasp that can resist tensile and shear forces.

The static model of the fruit clamping region is derived from Fig. 3-*Right*. The crank-slider linkage parameters are $d_1 = 47$ mm, $d_2 = 31$ mm, $d_3 = 90$ mm, $d_4 = 7$ mm, $d_5 = 18.5$ mm, $d_6 = 17.5$ mm, and $d_7 = 12$ mm. Equations (1)–(3), which use the laws of cosines and sines, describe the crank-slider linkage configuration as the nut moves a distance m along the lead-screw (here $z = d_3 - d_4 - m$):

$$\gamma = \cos^{-1}\left(\frac{{d_5}^2 + {d_6}^2 - {d_7}^2 - z^2}{2 d_5 d_6}\right) \tag{1}$$

$$\alpha = \tan^{-1}\left(\frac{d_7}{z}\right) \tag{2}$$

IEEE Robotics and Automation Letters (RA-L) paper, presented at ICRA 2026, Vienna, Austria. Cite as RA-L paper.

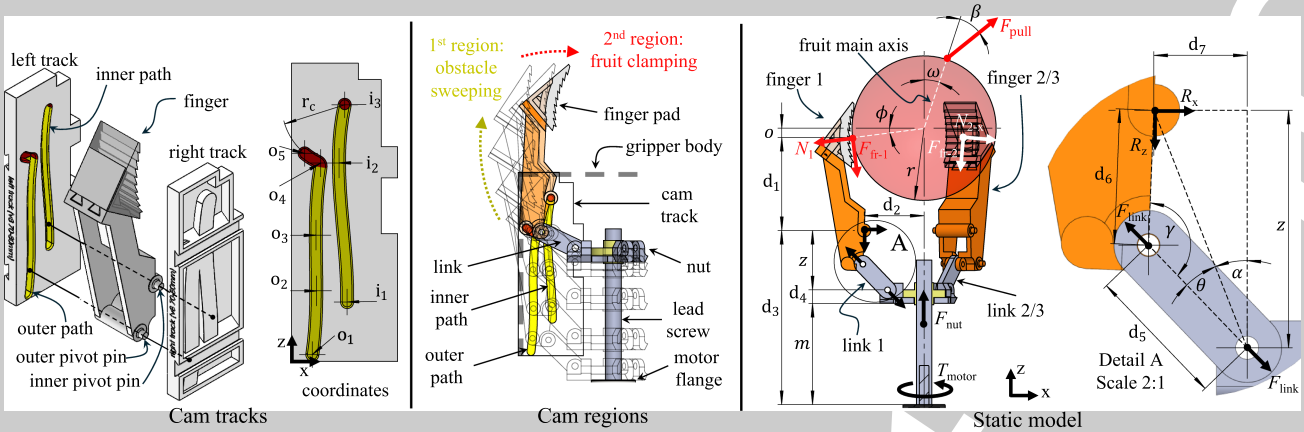

Fig. 3. Cam-driven finger mechanism. *Left:* Exploded view of a single finger and cam tracks, and coordinates of control points for outer and inner paths. The finger's outer pivot pin slides along the outer path of the tracks and the inner pivot pin slides along the inner path. *Middle:* Side view of the resulting path followed by the telescoping fingers – the fingers first curve outwards (yellow areas of the paths) to sweep obstacles away from the targeted fruit before moving inwards (red areas of the paths) to secure the fruit. *Right:* Detail view of linkage at the fruit clamping region with the geometric configuration of the force transmission model.

$$\theta = \sin^{-1}\left(\frac{\mathrm{d}_6 \cdot \sin\gamma}{\sqrt{{\mathrm{d}_7}^2 + z^2}}\right) \tag{3}$$

We use a stepper motor (Nema 17 - PHB 42S 34, bipolar with two stacks) that delivers a holding torque of 0.32 N m (T_{motor}). Power is transmitted to the crank-slider using a Tr8x8 lead screw with pitch $\mathrm{p_s} = 2$ mm, number of starts $\mathrm{n_s} = 4$, acme thread angle $\varphi = 14.5\,^\circ$, mean diameter $\mathrm{d_m} = 7$ mm, and screw-nut friction coefficient $\mu_{s2} = 0.2$. Equations (4)–(6) sequentially describe the force transmission from the motor to the nut F_{nut} [20], then to each link F_{link}, and finally to each finger pad F_{clamp}. Equation (7) summarizes the clamping force F_{clamp} at each finger, accounting for the number of links ($\mathrm{n_f} = 3$) and efficiency η.

$$F_{\text{nut}} = \left[\frac{2\left(\pi \mathrm{d_m} - \mu_{s2}\mathrm{p_s n_s}\sec\varphi\right)}{\mathrm{d_m}\left(\pi \mathrm{d_m}\mu_{s2}\sec\varphi + \mathrm{p_s n_s}\right)}\right] \cdot T_{\text{motor}} \tag{4}$$

$$F_{\text{link}} = \frac{1}{\mathrm{n_f} \cdot \cos(\alpha + \theta)} \cdot F_{\text{nut}} \tag{5}$$

$$F_{\text{clamp}} = \frac{\mathrm{d_6} \cdot \sin\gamma}{\mathrm{d_1}} \cdot F_{\text{link}} \tag{6}$$

$$F_{\text{clamp}} = \frac{\eta \mathrm{d_6}\sin\gamma}{\mathrm{n_f d_1}\cos(\alpha+\theta)}\left[\frac{2\left(\pi \mathrm{d_m} - \mu_{s2}\mathrm{p_s n_s}\sec\varphi\right)}{\mathrm{d_m}\left(\pi \mathrm{d_m}\mu_{s2}\sec\varphi + \mathrm{p_s n_s}\right)}\right] \cdot T_{\text{motor}} \tag{7}$$

The gain between the clamping force F_{clamp} and the thrust force at the lead-screw nut F_{nut} is shown in Fig. 4. As the linear displacement m increases, the angle $(\alpha + \theta)$ between the link and lead-screw also increases, leading to a corresponding rise in gain. To remain within the linear operating range, we limit m to 59 mm.

The following analysis describes the wrenches acting on the fruit and fingers, assuming that: (i) gravity is neglected; (ii) the fruit is modeled as a sphere; (iii) all contacts are assumed to be point, frictional, and rigid [21], [22]; (iv) the pulling force F_{pull} acts in a plane midway between fingers 2 and 3, allowing the forces on those fingers to be treated symmetrically; and (v) the system's indeterminacy is resolved using the superposition method to compute finger reaction forces. The angle formed by the offset o between the finger contact point and the fruit center is

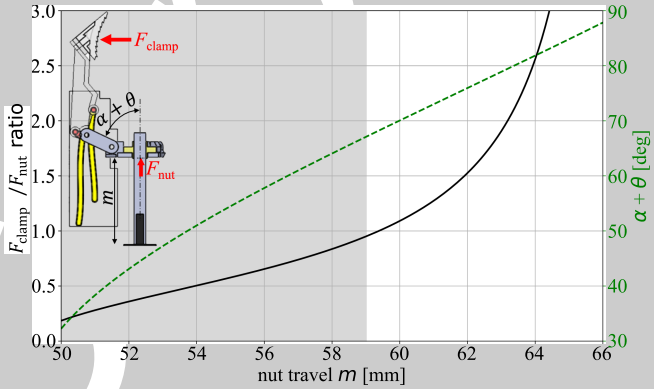

Fig. 4. Crank-slider linkage force ratio as a function of lead-screw nut travel m. The *solid* black curve shows the ratio of the normal clamping force F_{clamp} to the thrust force at the lead-screw nut F_{nut}. Motion is limited to 59 mm (gray-shaded area) to maintain linear behavior. The *dashed* green curve shows the angle $\alpha + \theta$, with force ratio increasing rapidly as this angle approaches 90 °.

$\phi = \sin^{-1}(\frac{o}{r})$. The equilibrium of the grasp is $\boldsymbol{x} = \boldsymbol{A}^{-1}\boldsymbol{b}$ where the vector $\boldsymbol{x}$ (8) consists of N_i, $F_{\text{fr-}i}$, and $F_{\text{link-}i}$, which represent the normal, friction, and link forces at each finger i, respectively, as well as F_{nut}, the thrust force at the lead-screw nut, and F_{pull}, the applied pulling force, (9) shown at the bottom of the next page.

$$\boldsymbol{x} = \begin{bmatrix} N_1 & F_{\text{fr-1}} & F_{\text{link-1}} & N_2 & F_{\text{fr-2}} & F_{\text{link-2}} & F_{\text{nut}} & F_{\text{pull}} \end{bmatrix}^T \tag{8}$$

$$\boldsymbol{b} = \begin{bmatrix} F_{\text{clamp}} & F_{\text{clamp}} & 0 & 0 & 0 & 0 & 0 & 0 \end{bmatrix}^T \tag{10}$$

IV. Evaluation and Validation

We evaluated the gripper through a combination of lab experiments and real apple-picking trials in a commercial orchard. First, we measured the clamping force on a near-spherical apple proxy (Section IV-A). We then analyzed grasp strength across three actuation modes—suction, fingers, and tandem— while varying the apple's pose relative to the gripper (Section IV-B). To test clutter robustness, we performed 34 fruit picks using

TABLE I
GRASP STRENGTH TESTS PERFORMED WITH A LOAD CELL

Variable	β [°]	Values	Mode	Reps	Total
Offset o [mm]	0	0, 5, 10, 15, 20	f	5	25
Angle ω [°]	0	0, 15, 30, 45	s, f, t	5	60
Angle ω [°]	90	0, 15, 30, 45	s, f, t	5	60

Actuation modes: s = suction, f = fingers, t = tandem

a physical proxy [8] with added leaves and apple clusters (Section IV-C). Finally, we conducted a real-world trial in a commercial orchard (Section IV-D).

A. Clamping Test

We measure the inward force F_{clamp} applied by the fingers to the fruit to validate the physical model described in Section III-C. Fig. 5 *(Bottom-left)* shows the experimental setup, where two fingers were constrained and the third applied force against a load cell (MR03-100). We record 10 samples per finger.

B. Grasp Strength Test

We measure grasp strength as the force required to pull an apple proxy (radius $r = 37.5\,\text{mm}$) from the gripper's grasp. This force will vary with the position of the apple in the gripper and the direction of pull from the stem. Our tests capture this variation as follows (see Table I): *Fruit offset* controls the displacement o of the apple from the palm (bigger displacements mean the fingers contact *below* the fruit equator). We varied the apple equator's starting position relative to the fingerpad center in $5\,\text{mm}$ steps from $0\,\text{mm}$ to $20\,\text{mm}$ (Fig. 5-*Top-left*). *Gripper to fruit angle* controls the angle ω between the gripper and the fruit main axis, while keeping the latter aligned with the pull direction ($\beta = 0\,^\circ$). The fruit main axis and pull direction pair are rotated in increments of $15\,^\circ$ from $0\,^\circ$ to $45\,^\circ$ (Fig. 5-*Middle*). *Rotational pull* evaluates the resistance to *rotational* force applied to the fruit. Here we also control the angle ω, but with a pull direction orthogonal to the fruit main axis ($\beta = 90\,^\circ$), simulating a force that would rotate the fruit to pull it out of the gripper (Fig. 5-*Right*). To conduct the tests, we used a materials testing machine (Mark10-ESM1500) with a load cell (MR03-100) mounted on the moving fixture, while keeping the gripper fixed (Fig. 5-*Middle* and 5-*Right*). One end of an inextensible fishing line was tied to the load cell and the other end to the apple proxy on the gripper's palm. For each trial, the gripper first grasped the fruit, then the fixture moved upward at 100 mm/min until the apple was pulled free. Tests were performed with three actuation modes—suction, fingers, and tandem—to isolate their effects. To validate our model we use a friction coefficient $\mu_{s1} = 0.8 \pm 0.1$ [13].

C. Clutter Test

We integrated the gripper with a UR5e manipulator (Universal Robots, Odense, Denmark) and used a physical apple proxy [8] designed to mimic the kinematic and dynamic behavior of an apple and stem. The proxy was configured with a 16 N FDF and a $455\,\text{N/m}$ branch stiffness, which are median values observed in real apple picks. The fake apples had a 75 mm diameter and were filled with sand to approximate the mass of Envy-type apples 200 ± 15 g. We evaluated different gripper poses by varying its pitch angle in 15° increments, from 0° (under the apple calyx) to 120° (above the fruit equator), following [7]. For the first clutter test, we arranged a cluster of three apples adjacent to each other and picked the middle one. In the second test, we increased complexity by adding fake leaves around the middle apple (Fig. 6-*Left*).

D. Field Trials

We used the same robotic system from Section IV-C and evaluated its performance in a commercial apple orchard (Prosser, WA; variety: 'Envy') during Fall 2023. These tests focused on the gripper only and excluded perception, path planning, etc. that would be required in a complete harvesting system. Each targeted apple and its stem were first probed to measure its ground truth pose as shown in Fig. 6-*Middle*. Following the method described in [8], we defined a pick direction v and an estimated apple center p (relative to the true apple center and stem direction). The gripper palm was placed 5 cm away from the targeted apple ($p - 5$ v), oriented along the pick direction v (Fig. 6-*Right*). The gripper was moved along v until either two suction cups engaged or a distance of 5 cm was reached. The fingers were subsequently actuated. The pick motion was a simple pull-back along $-v$ until the fruit detached or the grasp failed. For each trial, we recorded the manipulator's joint angles and wrist wrench measurements. Every attempt was performed without modifying the environment. Table II summarizes clutter and field trials. All equipment, including the laptop, UR5e manipulator, gripper, and 120 V air compressor, were powered from a 2048 Wh / 2400 W portable power station.

$$A = \begin{bmatrix} 1 & 0 & 0 & 0 & 0 & 0 & 0 & 0 \\ 0 & 0 & 0 & 1 & t\phi & 0 & 0 & -\frac{s(\omega+\beta)}{c\phi} \\ -s\phi & c\phi & 0 & -2s\phi & 2c\phi & 0 & 0 & -c(\omega+\beta) \\ 0 & -1 & 0 & 0 & 1 & 0 & 0 & s\beta \\ -\mathrm{d}_1 & r-\mathrm{d}_2 & \mathrm{d}_6 s\gamma & 0 & 0 & 0 & 0 & 0 \\ 0 & 0 & 0 & -\mathrm{d}_1 & r-\mathrm{d}_2 & \mathrm{d}_6 s\gamma & 0 & 0 \\ 0 & 0 & c(\alpha+\theta) & 0 & 0 & 2c(\alpha+\theta) & -1 & 0 \\ \mu_{s1} & -1 & 0 & 0 & 0 & 0 & 0 & 0 \end{bmatrix}$$

$$Note: s = \sin, c = \cos, \; t = \tan. \tag{9}$$

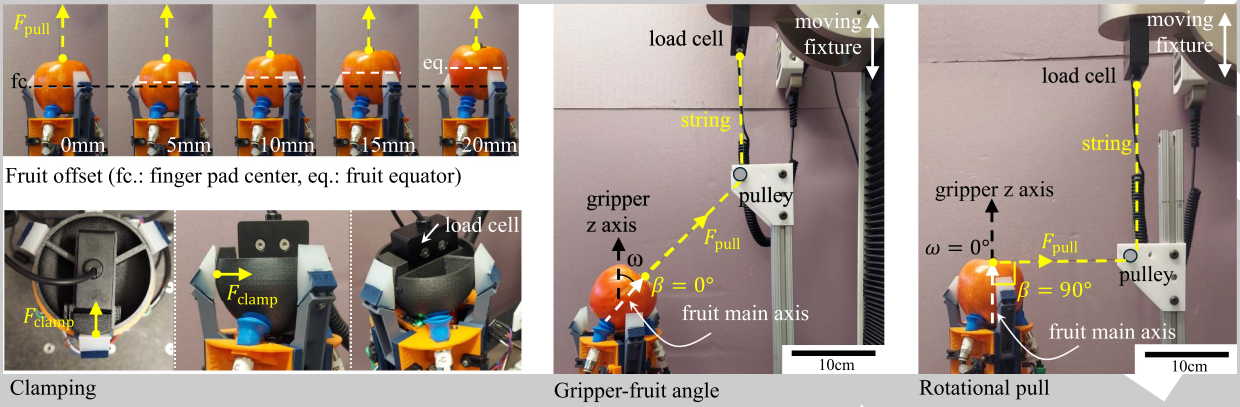

Fig. 5. Load cell tests. *Top-left:* Grasp strength test with different fruit offsets. *Bottom-left:* Setup used to measure the normal force F_{clamp} exerted by an individual finger. *Middle:* Grasp strength test with the apple main axis and string aligned ($\beta = 0°$), but varying the gripper-fruit angle ω. *Right:* Grasp strength test with the apple main axis aligned with the gripper ($\omega = 0°$) and the string oriented at $\beta = 90°$, inducing a rotational moment.

Fig. 6. *Left:* Trials using the physical apple proxy from [8] tuned to the median stem-detachment force and branch stiffness observed during field trials. *Middle:* Procedure used to capture the ground truth of the apple pose with a probe attached to the wrist of the manipulator. *Right:* Two samples of the apple pick trials in the field, with approach and pull-back vectors. Notice the fruit occlusion.

TABLE II
FRUIT-PICK TRIALS WITH GRIPPER AND UR5E MANIPULATOR

Exp.	Domain	Mode	Trials	Success [%]
1	Proxy (clusters)	t	9	100
2	Proxy (clusters + leaves)	t	25	96
3	Orchard	s	10	10
4	Orchard	t	26	81

Actuation modes: s = suction, f = fingers, t = tandem

V. RESULTS AND DISCUSSION

Our experimental results showed that tandem actuation, i.e. suction + fingers, significantly increased grasp strength for all test conditions. Moreover, our model predicted the behavior of the finger grasp strength. The total time to actuate the gripper, from initiation of suction to the fingers hitting their mechanical limits, is 1.5 sec. Additionally, the clutter trials showed that the telescoping fingers are effective at 'pushing' away neighboring fruit in clusters. Finally, during field trials, the apple pick success rate was 81%.

A. Clamping Test

The clamping forces F_{clamp} measured at the three fingers were 5.2 $\pm$ 1.3 N, 8.3 $\pm$ 2.8 N, and 10.0 $\pm$ 1.6 N, with an overall average of 8.0 $\pm$ 2.8 N. We attribute the variability across the three fingers to the difficulty of manually aligning the load cell orthogonally to the fingerpads. By comparing this result with (7), the approximate system efficiency η is 0.2, likely due to the tolerances in manufacturing, the elastic deformation of the components, and motor step skipping.

B. Grasp Strength Test

Fruit offset: Fig. 7-*Left* shows the force exerted by the gripper at various offsets for each actuation mode. In suction mode, the grasp strength from the three suction cups remains constant at 12.0 N, below the median FDF. With fingers only, the grasp strength exceeds the median FDF at zero offset but decreases with increasing offset, from 22.8 $\pm$ 2.5 N at 0 mm to 7.8 $\pm$ 1.5 N at 20 mm. The predictions of the finger model show similar trends and indicate that, for offsets exceeding 10 mm, the finger-only mode does not generate sufficient force. In contrast, with tandem actuation, the grasp strength exceeds the median FDF even at a 20 mm offset.

Gripper to fruit angle: Fig. 7-*Middle* shows that grasp strength increases with angle ω. In tandem mode, it rises from 34.5 $\pm$ 1.6 N at 0° to 39 $\pm$ 5.5 N at 45°. In fingers-only mode, it increases from 22.8 $\pm$ 2.5 N to 29.7 $\pm$ 7 N over the same range, closely matching the finger model predictions. We hypothesize that larger ω results in greater normal forces from the fingers, improving grasp strength. In both cases, the fingers alone are sufficient to counteract the median FDF.

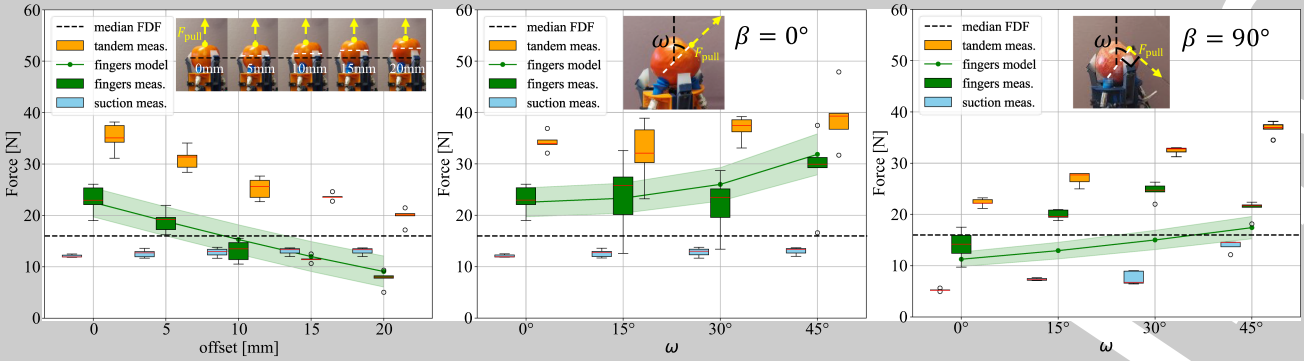

Fig. 7. Results from grasp strength tests alongside predicted values from static finger model. Model range is represented by the upper and lower bounds of the friction coefficient μ_{s1}. *Left:* Grasp strength for fruit offset vs actuation mode. *Middle:* Grasp strength vs gripper-fruit angle ω of pull force. *Right:* Grasp strength vs gripper-fruit angle ω with an orthogonal ($\beta = 90\,^\circ$) rotational pull. The dashed black line indicates the FDF for reference.

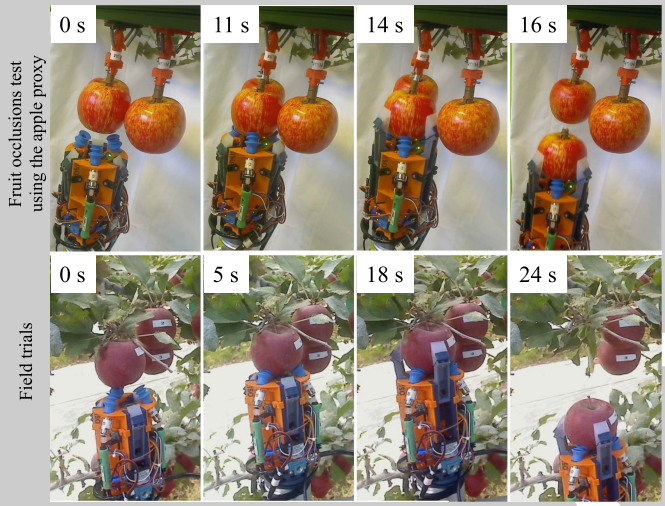

Fig. 8. Fruit pick sequence with elapsed time. *Top:* Sequence of the gripper picking the middle apple using the physical proxy. *Bottom:* Example field trial (cluster). While the gripper's uninterrupted cycle time is 1.5 sec, during these experiments the system was paused at various points to manually record data.

TABLE III
SUMMARY STATISTICS FROM FIELD TRIALS

Var.	n	Min	Q1	Med	Q3	Max
Fruit diameter [mm]	24	70	76	78	81	86
Fruit height [mm]	24	61	70	73	75	79
Fruit weight [g]	21	181	222	235	248	284
Net FDF [N]	22	7	11	15	28	38
Tangential FDF [N]	22	1	3	7	19	31
Normal FDF [N]	22	-2	7	12	19	33
Stiffness [N/m]	34	71	234	410	780	1324
Misalignment [mm]	39	1	5	10	16	30

Note: n is the sample size. Min = minimum, Q1 = first quartile, Med. = median, Q3 = third quartile, Max = maximum.

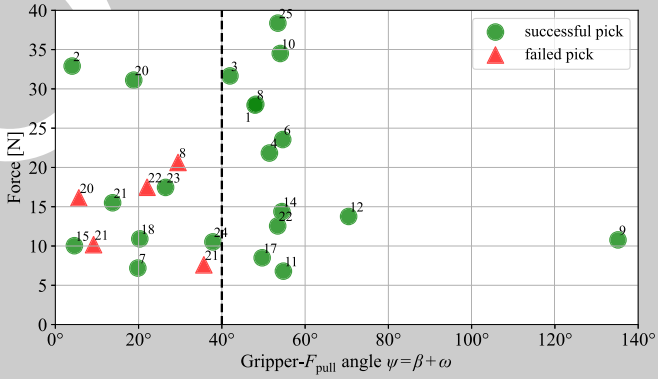

Fig. 9. Pulling force (F_{pull}) vs. Gripper-F_{pull} angle ($\psi = \omega + \beta$) for successful and failed apple picks during field trials using the gripper in tandem mode. All attempts with a $\psi > 40\,^\circ$ (dashed line) succedded. Labels indicate apple IDs. Notice how pick attempts of apples 8 and 22 initially failed, and then succeed with a larger ψ.

Rotational pull: Fig. 7-*Right* shows boxplots of grasp strength under rotational pull ($\beta = 90°$, and $\omega = 0°, 15°, 30°, 45°$) for each actuation mode. As in previous tests, suction mode alone remains below the median FDF across all ω values. Fingers mode yields its lowest strength of 14.0 ± 2.8 N at $\omega = 0°$, and increases with ω, peaking before dropping to 21.1 ± 1.7 N at $\omega = 45°$. This drop is likely due to the apple's asymmetry and finger 1's proximity to the apple south pole. In contrast, suction strength increases at $\omega = 45°$ to 13.9 ± 1.1, likely because the pull pushes the fruit against the suction cups. Overall, tandem strength consistently increases with ω. Finally, the finger model predictions align well with observations.

C. Clutter Lab Trials

For clustered apples (no leaves) we achieved a 100% success rate (9 trials). As shown in Fig. 8-*Top*, wedge-shaped fingers effectively moved the neighboring fruit away. When we added leaves, we succeeded in 24 of the 25 trials. In the failed trial, we observed that the leaves interfered with one of the suction cups.

D. Field Trials

We first attempted picking apples with just suction cups, then in tandem mode. For both modes we used the same modular cam track, which was selected based on the average diameter of Envy apples. A different cam track would need to be installed for picking substantially smaller or larger apples. Note that the pick motion was simply a pull-back – no attempt was made to perform a 'smarter' pick motion. A summary of the statistics of fruit properties, FDF, branch stiffness, and gripper x-axis offset relative to the fruit is shown in Table III.

During *suction mode*, the gripper achieved good initial grasps, but the suction cups failed before the apple was picked. This was expected, since the grasping force from the suction cups is not sufficient. Only one of our 10 pick attempts was successful. In contrast, with *tandem mode*, the pick-attempt success rate was 81%. A total of 17 apples were picked in the $1st$ attempt, two apples in the $2nd$ attempt, and one in the $3rd$ attempt. The median FDF was 15 N, close to our initial reference values; however, values up to 38 N were observed (Table III).

Fig. 9 shows the maximum net force at the manipulator's wrist plotted against the force angle ($\omega + \beta$) for field trials with tandem mode. There is no clear trend along the vertical axis (F_{pull}), as both failed and successful picks span the full force range—likely due to slippage from field-specific factors such as surface friction or object shape. In contrast, a clear trend appears along the horizontal axis: all failed trials occurred when the gripper-force angle was below 40°, whereas every attempt with a wider angle was successful. This suggests that the gripper is more robust to field-induced variations when the applied force vector exceeds $40\,^{\circ}$. A time sequence from one field trial is shown in Fig. 8-*Bottom*.

VI. Conclusion

In this work, we developed and evaluated a compact tandem-actuated gripper designed for selective apple harvesting, featuring both suction and cam-driven finger actuation. Experimental results demonstrated a maximum grasping strength of up to $40\,\text{N}$ across various fruit-gripper poses. Additionally, our tests with a physical apple proxy confirmed the gripper's robustness in handling fruit clusters and leaves, achieving a pick success rate above 96%. Field validation in a commercial apple orchard further confirmed the gripper's efficacy, with 21 out of 26 pick-attempts successfully achieved. Future work will focus on implementing an air-pressure-based servoing controller to enhance the engagement of the suction cups, optimizing the cam-tracks to accommodate a wider range of fruit diameters, and replacing the stepper motor with a servo motor to enhance efficiency.

Acknowledgment

The primary author thanks Fulbright-Colombia and Mincie ncias-Colombia for their financial support. We also thank Allan Bros., Inc. for supporting our field experiments in their commercial orchard.

References

[1] Z. Zhang, C. Igathinathane, J. Li, H. Cen, Y. Lu, and P. Flores, "Technology progress in mechanical harvest of fresh market apples," *Comput. Electron. Agriculture*, vol. 175, May 2020, Art. no. 105606.

[2] G. Kootstra, X. Wang, P. M. Blok, J. Hemming, and E. Van Henten, "Selective harvesting robotics: Current research, trends, and future directions," *Curr. Robot. Rep.*, vol. 2, no. 1, pp. 95–104, Mar. 2021.

[3] R. Lu, N. Dickinson, K. Lammers, K. Zhang, P. Chu, and Z. Li, "Design and evaluation of end effectors for a vacuum-based robotic apple harvester," *J. ASABE*, vol. 65, no. 5, pp. 963–974, 2022.

[4] J. Li, M. Karkee, Q. Zhang, K. Xiao, and T. Feng, "Characterizing apple picking patterns for robotic harvesting," *Comput. Electron. Agriculture*, vol. 127, pp. 633–640, 2016.

[5] W. Ji, G. He, B. Xu, H. Zhang, and X. Yu, "A new picking pattern of a flexible three-fingered end-effector for apple harvesting robot," *Agriculture*, vol. 14, no. 1, Jan. 2024, Art. no. 102.

[6] J. Tong, Q. Zhang, M. Karkee, H. Jiang, and J. Zhou, "Understanding the dynamics of hand picking patterns of fresh market apples," in *Proc. Amer. Soc. Agricultural Biol. Engineers*, 2014, pp. 2057–2063.

[7] A. Velasquez, C. Grimm, and J. R. Davidson, "Dynamic evaluation of a suction based gripper for fruit picking using a physical twin," in *Proc. IEEE Int. Conf. Robot. Automat.*, 2024, pp. 11839–11845.

[8] A. Velasquez, N. Swenson, M. Cravetz, C. Grimm, and J. R. Davidson, "Predicting fruit-pick success using a grasp classifier trained on a physical proxy," in *Proc. IEEE/RSJ Int. Conf. Intell. Robots Syst.*, 2022, pp. 9225–9231.

[9] J. F. Elfferich, D. Dodou, and C. D. Santina, "Soft robotic grippers for crop handling or harvesting: A review," *IEEE Access*, vol. 10, pp. 75428–75443, 2022.

[10] C. J. Hohimer, H. Wang, S. Bhusal, J. Miller, C. Mo, and M. Karkee, "Design and field evaluation of a robotic apple harvesting system with a 3D-printed soft-robotic end-effector," *Trans. ASABE*, vol. 62, no. 2, pp. 405–414, 2019.

[11] P. Boyraz, G. Runge, and A. Raatz, "An overview of novel actuators for soft robotics," *High-Throughput*, vol. 7, no. 3, pp. 1–21, 2018.

[12] C.-H. Liu, F.-M. Chung, Y. Chen, C. -H. Chiu, and T.-L. Chen, "Optimal design of a motor-driven three-finger soft robotic gripper," *IEEE/ASME Trans. Mechatron.*, vol. 25, no. 4, pp. 1830–1840, Aug. 2020.

[13] K. Chen et al., "A soft gripper design for apple harvesting with force feedback and fruit slip detection," *Agriculture*, vol. 12, no. 11, Oct. 2022, Art. no. 1802.

[14] C. Chi et al., "Universal manipulation interface: In-the-wild robot teaching without in-the-wild robots," in *Proc. Robot.: Sci. Syst.*, Delft, Netherlands, Jul. 2024.

[15] W. Hua et al., "Vacuum suction end-effector development for robotic harvesters of fresh market apples," *Biosyst. Eng.*, vol. 249, pp. 28–40, Jan. 2025.

[16] M. Wang et al., "Development of a novel biomimetic mechanical hand based on physical characteristics of apples," *Agriculture*, vol. 12, no. 11, Nov. 2022, Art. no. 1871.

[17] X. Wang, H. Kang, H. Zhou, W. Au, M. Y. Wang, and C. Chen, "Development and evaluation of a robust soft robotic gripper for apple harvesting," *Comput. Electron. Agriculture*, vol. 204, Jan. 2023, Art. no. 107552.

[18] Q. Vu and A. Ronzhin, "A model of four-finger gripper with a built-in vacuum suction nozzle for harvesting tomatoes," in *Proc. 14th Int. Conf. Electromechanics Robot. "zavalishin's Readings*, Singapore, A. Ronzhin and V. Shishlakov, Eds., 2020, pp. 149–160.

[19] A. Pagoli, F. Chapelle, J. A. Corrales, Y. Mezouar, and Y. Lapusta, "A soft robotic gripper with an active palm and reconfigurable fingers for fully dexterous in-hand manipulation," *IEEE Robot. Automat. Lett.*, vol. 6, no. 4, pp. 7706–7713, Oct. 2021.

[20] J. E. Shigley, *Mechanical Engineering Design*, 8th ed.. New York, NY, USA: McGraw-Hill Education, 2021.

[21] W. S. Howard and V. Kumar, "On the stability of grasped objects," *IEEE Trans. Robot. Automat.*, vol. 12, no. 6, pp. 904–917, Dec. 1996.

[22] A. Bicchi and V. Kumar, "Robotic grasping and contact: A review," in *Proc. IEEE Int. Conf. Robot. Automat.*, San Francisco, CA, USA, 2000, vol. 1, pp. 348–353.